

Thermodynamics of $SU(3)$ Gauge Theory from Gradient Flow

Masayuki Asakawa,^{1,*} Tetsuo Hatsuda,^{2,3,†} Etsuko Itou,^{4,‡} Masakiyo Kitazawa,^{1,§} and Hiroshi Suzuki^{5,¶}
(FlowQCD Collaboration)

¹*Department of Physics, Osaka University, Toyonaka, Osaka 560-0043, Japan*

²*Theoretical Research Division, Nishina Center, RIKEN, Wako 351-0198, Japan*

³*Kavli IPMU (WPI), The University of Tokyo, Chiba 606-8502, Japan*

⁴*High Energy Accelerator Research Organisation (KEK), Tsukuba 305-0801, Japan*

⁵*Department of Physics, Kyushu University, 6-10-1 Hakozaki, Higashi-ku, Fukuoka, 812-8581, Japan*

A novel method to study the bulk thermodynamics in lattice gauge theory is proposed on the basis of the Yang–Mills gradient flow with a fictitious time t . The energy density ε and the pressure P of $SU(3)$ gauge theory at fixed temperature are calculated directly on $32^3 \times (6, 8, 10)$ lattices from the thermal average of the well-defined energy-momentum tensor $T_{\mu\nu}^R(x)$ obtained by the gradient flow. It is demonstrated that the continuum limit can be taken in a controlled manner from the t -dependence of the flowed data.

PACS numbers: 05.70.Ce; 11.10.Wx; 11.15.Ha

The symmetric energy momentum tensor (EMT), $T_{\mu\nu}$, which is the generator of the Poincaré transformations, is a fundamental operator in quantum field theory [1]. Since T_{00} , T_{i0} , and T_{ij} correspond to the energy density, the momentum density, and the momentum-flux density, respectively, the EMT and its correlation functions provide useful information on the bulk and transport properties at finite temperature (T). For example, the energy density ε and the pressure P are given by $\langle T_{00} \rangle$ and $\langle T_{11,22,33} \rangle$, respectively, with $\langle \cdot \rangle$ being the thermal average. Also, the shear viscosity η can be extracted from the two-point correlation, $\langle T_{12}(x)T_{12}(y) \rangle$. In quantum chromodynamics (QCD), these observables are particularly important in formulating the relativistic hydrodynamics for the quark-gluon plasma [2]. Therefore, high precision and non-perturbative evaluation of the n -point EMT correlations in lattice QCD is called for.

To calculate such correlations in numerical lattice simulations, we first need to define proper EMT on the lattice which is ultra-violet (UV) finite and is conserved in the continuum limit. Such a construction is not a trivial task due to the explicit breaking of the Poincaré invariance on the lattice. (See Refs. [3–6] for recent developments.) This is the reason why ε and P at finite T have been mainly studied by an indirect “integral method” without the explicit use of the EMT [7].

Very recently, one of the present authors has shown that the proper EMT keeping all the nice features can be naturally constructed [8] on the basis of the Yang–Mills gradient flow [9–11]. (See also related works, Refs. [12–16].) The main purpose of the present Letter is to demonstrate that the thermodynamics of the $SU(3)$ gauge theory can be indeed studied with high accuracy with modest statistics by the direct use of the EMT obtained from the gradient flow. The key idea is to represent the EMT in the continuum limit in terms of UV-finite and local operators obtained from the gradient flow. Then, by taking the limit of small flow time and small lattice spacing in an

appropriate way, which will be discussed later, accurate thermodynamic observables are obtained.

Let us first recapitulate the basic idea of Ref. [8] in the continuum space-time. The Yang–Mills gradient flow is a deformation of the gauge configuration $A_\mu(x)$ along a fictitious Euclidean time t ,

$$\partial_t B_\mu(t, x) = D_\nu G_{\nu\mu}(t, x), \quad B_\mu(t=0, x) = A_\mu(x), \quad (1)$$

where D_μ and $G_{\mu\nu}(t, x)$ are the covariant derivative and the field strength of the flowed gauge field $B_\mu(t, x)$, respectively. The color indices are suppressed for simplicity. A salient feature of the gradient flow is its UV finiteness: Any correlation functions of $B_{\mu_1}(t_1, x_1)$, $B_{\mu_2}(t_2, x_2)$, \dots for $t_i > 0$ are UV finite without the wave function renormalization if they are written in terms of the renormalized coupling [10]. This is owing to the fact that the diffusion in t naturally introduces a proper-time regulator of the form e^{-tp^2} , where p denotes a typical loop momentum. In particular, the correlation functions are free from UV divergences even at the equal-point, $(t_1, x_1) = (t_2, x_2) = \dots$ for positive t_i . For example, the following gauge-invariant local products of dimension 4 are UV finite for $t > 0$: $U_{\mu\nu}(t, x) \equiv G_{\mu\rho}(t, x)G_{\nu\rho}(t, x) - \frac{1}{4}\delta_{\mu\nu}G_{\rho\sigma}(t, x)G_{\rho\sigma}(t, x)$ and $E(t, x) \equiv \frac{1}{4}G_{\mu\nu}(t, x)G_{\mu\nu}(t, x)$.

For $t \rightarrow 0_+$, local products of flowed fields can be expanded in terms of four-dimensional renormalized local operators with increasing dimensions [10]: The expansion coefficients are governed by the renormalization group equation and their small t behavior can be calculated by perturbation theory thanks to the asymptotic freedom. For the operators mentioned above, we have [8, 17]

$$U_{\mu\nu}(t, x) = \alpha_U(t) \left[T_{\mu\nu}^R(x) - \frac{1}{4}\delta_{\mu\nu}T_{\rho\rho}^R(x) \right] + O(t), \quad (2)$$

$$E(t, x) = \langle E(t, x) \rangle_0 + \alpha_E(t)T_{\rho\rho}^R(x) + O(t), \quad (3)$$

where $\langle \cdot \rangle_0$ is vacuum expectation value and $T_{\mu\nu}^R(x)$ is

the correctly-normalized conserved EMT with its vacuum expectation value subtracted. Abbreviated are the contributions from the operators of dimension 6 or higher, which are suppressed for small t .

Combining relations Eqs. (2) and (3), we have

$$T_{\mu\nu}^R(x) = \lim_{t \rightarrow 0} \left\{ \frac{1}{\alpha_U(t)} U_{\mu\nu}(t, x) + \frac{\delta_{\mu\nu}}{4\alpha_E(t)} [E(t, x) - \langle E(t, x) \rangle_0] \right\}, \quad (4)$$

where the perturbative coefficients are found to be [8]

$$\alpha_U(t) = \bar{g}(1/\sqrt{8t})^2 \left[1 + 2b_0 \bar{s}_1 \bar{g}(1/\sqrt{8t})^2 + O(\bar{g}^4) \right], \quad (5)$$

$$\alpha_E(t) = \frac{1}{2b_0} \left[1 + 2b_0 \bar{s}_2 \bar{g}(1/\sqrt{8t})^2 + O(\bar{g}^4) \right]. \quad (6)$$

Here $\bar{g}(q)$ denotes the running gauge coupling in the $\overline{\text{MS}}$ scheme with the choice, $q = 1/\sqrt{8t}$, and $\bar{s}_1 = \frac{7}{16} + \frac{1}{2}\gamma_E - \ln 2 \simeq 0.032960651891$, $\bar{s}_2 = \frac{109}{176} - \frac{b_1}{2b_0^2} = \frac{383}{1936} \simeq 0.19783057851$, with $b_0 = \frac{1}{(4\pi)^2} \frac{11}{3} N_c$, $b_1 = \frac{1}{(4\pi)^4} \frac{34}{3} N_c^2$, and $N_c = 3$. Note that a non-perturbative determination of $\alpha_{U,E}(t)$ is also proposed recently [17].

The formula Eq. (4) indicates that $T_{\mu\nu}^R(x)$ can be obtained by the small t limit of the gauge-invariant local operators defined through the gradient flow. There are two important observations: (i) The right-hand side of Eq. (4) is independent of the regularization because of its UV finiteness, so that one can take, e.g. the lattice regularization scheme to make numerical simulations; (ii) since flowed fields at $t > 0$ depend on the fundamental fields at $t = 0$ in the space-time region of radius $\simeq \sqrt{8t}$, the statistical noise in calculating the right hand side of Eq. (4) is suppressed for finite t .

Let us split the procedure to calculate the EMT on the lattice into the following four steps:

Step 1: Generate gauge configurations at $t = 0$ on a space-time lattice with the lattice spacing a and the lattice size $N_s^3 \times N_\tau$.

Step 2: Solve the gradient flow for each configuration to obtain the flowed link variables in the fiducial window, $a \ll \sqrt{8t} \ll R$. Here, R is an infrared cutoff scale such as $\Lambda_{\text{QCD}}^{-1}$ or $T^{-1} = N_\tau a$. The first (second) inequality is necessary to suppress finite a corrections (non-perturbative corrections and finite volume corrections).

Step 3: Construct $U_{\mu\nu}(t, x)$ and $E(t, x)$ in Eqs. (2) and (3) in terms of the flowed link variables and average over the gauge configurations at each t .

Step 4: Carry out an extrapolation toward $(a, t) = (0, 0)$ according to Eq. (4) under the constraint, $a \ll \sqrt{8t}$.

The thermodynamic quantities, ε and P , are obtained from the diagonal elements of the EMT. In particular, a combination called the interaction measure Δ is related to the trace of the EMT (the trace anomaly):

$$\Delta = \varepsilon - 3P = -\langle T_{\mu\mu}^R(x) \rangle. \quad (7)$$

N_τ	6	8	10	T/T_c
	6.20	6.40	6.56	1.65
β	6.02	6.20	6.36	1.24
	5.89	6.06	6.20	0.99

TABLE I: Values of β and N_τ for each temperature.

Also, the entropy density s at zero chemical potential is written as

$$sT = \varepsilon + P = -\langle T_{00}^R(x) \rangle + \frac{1}{3} \sum_{i=1,2,3} \langle T_{ii}^R(x) \rangle. \quad (8)$$

To demonstrate that the above four Steps can be indeed pursued, we consider the $SU(3)$ gauge theory defined on a four-dimensional Euclidean lattice, whose thermodynamics has been extensively studied by the integral method [18–21]. For simplicity, we consider the Wilson plaquette gauge action under the periodic boundary condition on $N_s^3 \times N_\tau = 32^3 \times (6, 8, 10)$ lattices with several different $\beta = 6/g_0^2$ (g_0 being the bare coupling constant). Gauge configurations are generated by the pseudo-heatbath algorithm with the over-relaxation, mixed in the ratio of 1 : 5. We call one pseudo-heatbath update sweep plus five over-relaxation sweeps as a ‘‘Sweep’’. To eliminate the autocorrelation, we take 200–500 Sweeps between measurements. The number of gauge configurations for the measurements at finite T is 300. Statistical errors are estimated by the jackknife method.

To relate T/T_c and corresponding β for each N_τ , we first use the relation between a/r_0 (r_0 is the Sommer scale) and β given by the ALPHA Collaboration [22]. The resultant values of $Tr_0 = [N_\tau(a/r_0)]^{-1}$ are then converted to T/T_c by using the result at $\beta = 6.20$ in Ref. [18]. Nine combinations of (N_τ, β) and corresponding T/T_c obtained by this procedure are shown in Table I.

The gradient flow in the t -direction is obtained by solving the ordinary first-order differential equation. To increase its numerical accuracy and efficiency, the third-order Runge–Kutta method in Ref. [9] is generalized to a fourth-order one [23] in which the error per step ($t \rightarrow t + \epsilon$) is reduced to $O(\epsilon^5)$. We take $\epsilon = 0.025$ so that the accumulation errors become sufficiently smaller than the statistical errors. This fourth-order integrator turns out to be almost twice faster than the third-order one to reach the same t .

To extract the EMT from Eq. (4), we measure $G_{\mu\rho}^a(t, x) G_{\nu\rho}^a(t, x)$ written in terms of the clover leaf representation on the lattice. To subtract out the $T = 0$ contribution, $\langle E(t, x) \rangle_0$, we carry out simulations on a 32^4 lattice for each β in Table I. Note that this vacuum subtraction is required only for the measurement of the trace anomaly Δ , while no subtraction is needed for the measurement of the entropy density s . For \bar{g} in $\alpha_U(t)$ and

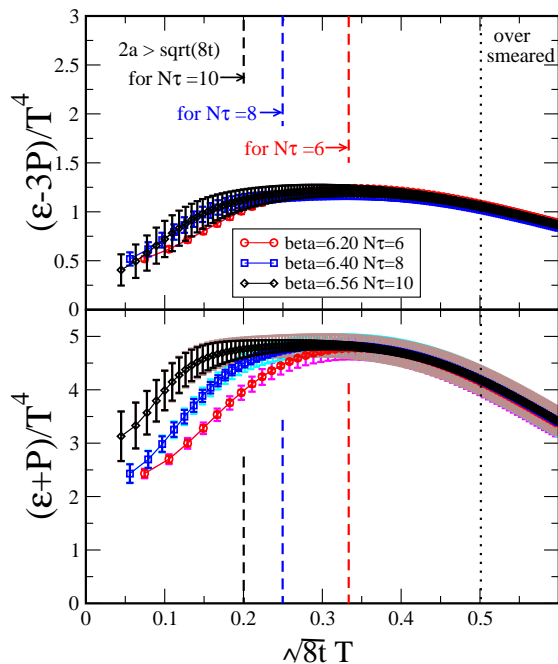


FIG. 1: Flow time dependence of the dimensionless interaction measure (top panel) and the dimensionless entropy density (bottom panel) for different lattice spacings at fixed $T/T_c = 1.65$. The circles (red) the squares (blue), and the diamonds (black) correspond to $N_\tau = 6, 8$, and 10 , respectively. The bold error bars denote the statistical errors, while the thin error bars (brown, cyan, and magenta) include both statistical and systematic errors.

$\alpha_E(t)$ given by Eqs. (5) and (6), we use the four-loop running coupling with the scale parameter determined by the ALPHA Collaboration, $\Lambda_{\overline{\text{MS}}} = 0.602(48)/r_0$ [24]. We confirmed the previous finding [9] that the lattice data of $t^2 \langle E(t, x) \rangle_0$ in the fiducial window matches quite well with its perturbative estimate in the continuum, $t^2 \langle E(t, x) \rangle_0 \simeq 3\bar{g}^2 / (4\pi)^2 [1 + 1.0978\bar{g}(1/\sqrt{8t})^2 / (4\pi)]$ with the four-loop running coupling and the above $\Lambda_{\overline{\text{MS}}}$.

Let us now show, in Fig. 1, our results for the dimensionless interaction measure ($\Delta/T^4 = (\varepsilon - 3P)/T^4$) and the dimensionless entropy density ($s/T^3 = (\varepsilon + P)/T^4$) at $T = 1.65T_c$ as a function of the dimensionless flow parameter $\sqrt{8t}T$. The bold bars denote the statistical errors, while the thin (light color) bars show the statistical and systematic errors including the uncertainty of $\Lambda_{\overline{\text{MS}}}$. We found that the statistical error is dominant in the small t region for both Δ/T^4 and s/T^3 , while the systematic error originating from the scale parameter becomes significant for s/T^3 in the large t region.

The fiducial window discussed in **Step 2** is indicated by the dashed lines in Fig. 1. The lower limit of the window, beyond which the lattice discretization error grows, is set to be $\sqrt{8t_{\min}} = 2a$, where we take into account the fact that our clover leaf operator extends the size $2a$. The

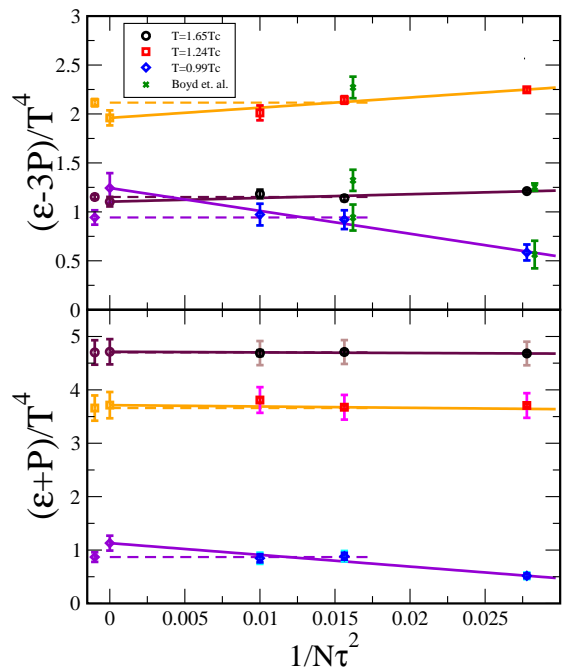


FIG. 2: Continuum extrapolation of the thermodynamic quantities for $T/T_c = 1.65, 1.24$, and 0.99 . Solid lines and dashed lines correspond to the three-point linear fit and two-point constant fit as a function of $1/N_\tau^2$, respectively. Extrapolated values of the former (latter) are shown at $1/N_\tau^2 = 0$ ($1/N_\tau^2 = -0.001$). The cross symbols in the top panel are the data of Ref. [18] with the same lattice setup.

upper limit of the window, beyond which the smearing by the gradient flow exceeds the temporal lattice size, is set to be $\sqrt{8t_{\max}} = 1/(2T) = N_\tau a/2$.

The data in Fig. 1 show, within the error bars, that (i) the plateau appears inside the preset fiducial window ($2/N_\tau < \sqrt{8t}T < 1/2$) for each N_τ , and (ii) the plateau extends to the smaller t region as N_τ increases or equivalently as a decreases. It should be remarked that only 300 gauge configurations are necessary to obtain these results. Similar plateaus as in Fig. 1 also appear inside the fiducial window for other temperatures, $T/T_c = 1.24$ and 0.99 , with comparable error bars. These features imply that our **Step 4** to take the double extrapolation $(a, t) \rightarrow (0, 0)$ is indeed possible.

Our lattice results at fixed T with three different lattice spacings allow us to take the continuum limit. First, we pick up a flow time $\sqrt{8t}T = 0.40$ which is in the middle of the fiducial window. Then we extract Δ/T^4 and s/T^3 for each set of N_τ and β . We have checked that different choices of t do not change the final results within the error bar as long as it is in the plateau region. In Fig. 2, resultant values taking into account the statistical errors (bold error bars) and the statistical plus systematic errors (thin error bars) are shown. The lattice data for Δ/T^4 with the same lattice setup at $N_\tau = 6$ and 8 in Ref. [18] are also

shown by the cross (green) symbols in the top panel; our results with 300 gauge configurations have substantially smaller error bars at these points.

The horizontal axis of Fig. 2, $1/N_\tau^2$, is a variable suited for making continuum extrapolation of the thermodynamic quantities [18]. We consider two ways of extrapolation: A linear fit with the data at $N_\tau = 6, 8$, and 10 (the solid lines in Fig. 2), and a constant fit with the data at $N_\tau = 8$ and 10 (the dashed lines in Fig. 2). In both fits, the correlation between the errors due to the common systematic error from $\Lambda_{\overline{\text{MS}}}$ is taken into account. The former fit is used to determine the central value in the continuum limit whose error is within $\pm 12\%$ even at our lowest temperature. The latter is used to estimate the systematic error from the scaling violation whose typical size is $\pm 4\%$ at high temperature and $\pm 24\%$ at low temperature.

We have analyzed various systematic errors; the perturbative expansion of $\alpha_{U,E}(t)$, the running coupling \bar{g} , the scale parameter, and the continuum extrapolation. We found that the dominant errors in the present lattice setup are those from $\Lambda_{\overline{\text{MS}}}$ and the continuum extrapolation, which are included in Fig. 2. To reduce these systematic errors, finer lattices are quite helpful: They make the plateau in $\sqrt{8t}T$ wider by reducing the lower limit of the fiducial window, so that the continuum extrapolation becomes easier. Also, larger aspect ratio N_s/N_τ would be helpful to guarantee the thermodynamic limit. Moreover, the scale setting procedure could be improved to have better accuracy: Instead of the Sommer scale r_0 adopted in this Letter, more precise scale determination, e.g. by t_0 or ω_0 in the gradient flow approach [9, 14], will be useful.

Finally, we plot, in Fig. 3, the continuum limit of Δ/T^4 and s/T^3 obtained by the linear fit of the $N_\tau = 6, 8$, and 10 data (the solid lines) in Fig. 2 for $T/T_c = 1.65, 1.24$, and 0.99. For comparison to the existing data with the same lattice setup, the results of Ref. [18] obtained by the integral method are shown by the grey lines in Fig. 3 in which Δ/T^4 for $N_\tau = 8$ and P/T^4 for $N_\tau = 6$ and 8 are adopted to estimate the continuum values. The results of the two different approaches are consistent with each other within 2 sigma level, which indicates that the method of the gradient flow indeed works already with 300 gauge configurations.

In this Letter, we have proposed a novel way to study the thermodynamics of the $SU(3)$ gauge theory on the lattice on the basis of the Yang–Mills gradient flow with the fictitious time t . The key ingredient is the conserved and UV-finite energy-momentum tensor $T_{\mu\nu}^R(x)$ defined from the $t \rightarrow 0$ limit of the UV-finite operators $(U_{\mu\nu}(t, x)$ and $E(t, x)$) with the matching coefficients $(\alpha_U(t)$ and $\alpha_E(t))$ [8]. From the simulations on $32^3 \times (6, 8, 10)$ lattices with modest statistics (300 gauge configurations), we found that the dimensionless interaction measure and entropy density, $(\varepsilon - 3P)/T^4$

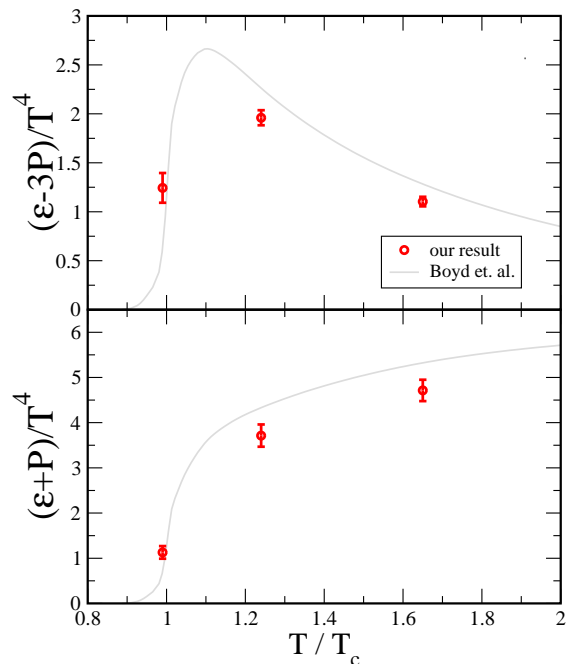


FIG. 3: Continuum limit of the interaction measure and entropy density obtained by the gradient flow for $T/T_c = 1.65, 1.24$, and 0.99 with 300 gauge configurations. The grey lines are the results of the integral method with typical error $\pm 2\%$ according to Fig. 7 of Ref. [18].

and $(\varepsilon + P)/T^4$, show plateau structure inside the fiducial window ($2/N_\tau < \sqrt{8t}T < 1/2$) with small statistical errors, so that the double limit $(a, t) \rightarrow (0, 0)$ can be taken appropriately for given T . Results obtained in the new method are qualitatively consistent with those obtained by the conventional integral method [18].

Major advantages of the gradient flow applied to the thermodynamics on the lattice are as follows: (i) One can simulate ε and P independently at any fixed T through the direct measurement of the well-defined EMT. There is no need of integration by β or T , which requires a boundary condition and the numerical interpolation. (ii) There is no need of constant subtraction in entropy density s . The interaction measure Δ needs one subtraction of its $T = 0$ value, which is obtained by the accurate measurement of $t^2 \langle E(t, x) \rangle_0$ or by its perturbative evaluation at small t . (iii) The statistical noise is substantially reduced at finite flow time $t > 0$ due to the effective smearing of the operators with the radius $\simeq \sqrt{8t}$, so that the extrapolation of the results back to $t = 0$ can be carried out in a well-controlled manner.

We considered only the thermal average of EMT in this Letter. However, there is no conceptual difficulties in applying our method to n -point correlations of EMTs [8]. This opens the door to investigate transport coefficients (such as shear and bulk viscosities), fluctuation observables in the hot plasma, glueballs at zero and finite tem-

peratures, and so forth. It should be noted that there is no difficulty in measuring thermodynamic quantities even at extremely high temperature in this method since no temperature integration is necessary. It is also an interesting direction to study the dilation mode or the a -function of (nearly) conformal theory [25, 26] using the present method. Furthermore, including fermions in the present framework extends the scope even further. Some of these issues as well as the simulations with finer lattice with larger volume are already started and will be reported elsewhere.

We would like to thank S. Aoki, F. Karsch, M. Lüscher, and H. Nagatani for useful discussions and comments. We are also grateful to H. Matsufuru for his help of the code development. Numerical simulation was carried out on NEC SX-8R and SX-9 at RCNP, Osaka University, and Hitachi SR16000 at KEK under its Large-Scale Simulation Program (Nos. T12-04 and 13/14-20). The work of M. A., M. K., and H. S. are supported in part by a Grant-in-Aid for Scientific Researches 23540307, 25800148, and 23540330, respectively. E. I. is supported in part by Strategic Programs for Innovative Research (SPIRE) Field 5. This work is partially supported by RIKEN iTHES Project.

* Electronic address: yuki@phys.sci.osaka-u.ac.jp

† Electronic address: thatsuda@riken.jp

‡ Electronic address: eitou@post.kek.jp

§ Electronic address: kitazawa@phys.sci.osaka-u.ac.jp

¶ Electronic address: hsuzuki@phys.kyushu-u.ac.jp

- [1] S. Caracciolo, G. Curci, P. Menotti and A. Pelissetto, *Annals Phys.* **197**, 119 (1990).
- [2] Reviewed in, P. Romatschke, *Int. J. Mod. Phys. E* **19**, 1 (2010) [arXiv:0902.3663 [hep-ph]].
- [3] L. Giusti and H. B. Meyer, *JHEP* **1301**, 140 (2013) [arXiv:1211.6669 [hep-lat]].
- [4] D. Robaina and H. B. Meyer, arXiv:1310.6075 [hep-lat].
- [5] L. Giusti and H. B. Meyer, arXiv:1310.7818 [hep-lat].
- [6] L. Giusti and M. Pepe, arXiv:1311.1012 [hep-lat].

- [7] Reviewed in, M. P. Lombardo, *PoS LATTICE* **2012**, 016 (2012) [arXiv:1301.7324 [hep-lat]].
- [8] H. Suzuki, *PTEP* **2013**, no. 8, 083B03 (2013) [arXiv:1304.0533 [hep-lat]].
- [9] M. Lüscher, *JHEP* **1008**, 071 (2010) [arXiv:1006.4518 [hep-lat]].
- [10] M. Lüscher and P. Weisz, *JHEP* **1102**, 051 (2011) [arXiv:1101.0963 [hep-th]].
- [11] Reviewed in, M. Lüscher, arXiv:1308.5598 [hep-lat].
- [12] S. Borsanyi, S. Dürr, Z. Fodor, C. Hoelbling, S. D. Katz, S. Krieg, T. Kurth and L. Lellouch *et al.*, *JHEP* **1209**, 010 (2012) [arXiv:1203.4469 [hep-lat]].
- [13] S. Borsanyi, S. Dürr, Z. Fodor, S. D. Katz, S. Krieg, T. Kurth, S. Mages and A. Schäfer *et al.*, arXiv:1205.0781 [hep-lat].
- [14] Z. Fodor, K. Holland, J. Kuti, D. Nogradi and C. H. Wong, *JHEP* **1211**, 007 (2012) [arXiv:1208.1051 [hep-lat]].
- [15] P. Fritzsche and A. Ramos, *JHEP* **1310**, 008 (2013) [arXiv:1301.4388 [hep-lat]].
- [16] M. Lüscher, *JHEP* **1304**, 123 (2013) [arXiv:1302.5246 [hep-lat]].
- [17] L. Del Debbio, A. Patella and A. Rago, *JHEP* **1311**, 212 (2013) [arXiv:1306.1173 [hep-th]].
- [18] G. Boyd, J. Engels, F. Karsch, E. Laermann, C. Legeland, M. Lutgemeier and B. Petersson, *Nucl. Phys. B* **469**, 419 (1996) [hep-lat/9602007].
- [19] M. Okamoto *et al.* [CP-PACS Collaboration], *Phys. Rev. D* **60**, 094510 (1999) [hep-lat/9905005].
- [20] T. Umeda, S. Ejiri, S. Aoki, T. Hatsuda, K. Kanaya, Y. Maezawa and H. Ohno, *Phys. Rev. D* **79**, 051501 (2009) [arXiv:0809.2842 [hep-lat]].
- [21] S. Borsanyi, G. Endrodi, Z. Fodor, S. D. Katz and K. K. Szabo, *JHEP* **1207**, 056 (2012) [arXiv:1204.6184 [hep-lat]].
- [22] M. Guagnelli *et al.* [ALPHA Collaboration], *Nucl. Phys. B* **535**, 389 (1998) [hep-lat/9806005].
- [23] E. Itou, in preparation.
- [24] S. Capitani *et al.* [ALPHA Collaboration], *Nucl. Phys. B* **544**, 669 (1999) [hep-lat/9810063].
- [25] T. Appelquist and Y. Bai, *Phys. Rev. D* **82**, 071701 (2010) [arXiv:1006.4375 [hep-ph]].
- [26] J. I. Latorre and H. Osborn, *Nucl. Phys. B* **511**, 737 (1998) [hep-th/9703196].